Theoretical and Applied Climatology
https://doi.org/10.1007/s00704-018-2586-2

ORIGINAL PAPER

Calibration and uncertainty analysis of a hydrological model based on cuckoo search and the M-GLUE method

Hongxue Zhang[1] · Jianxia Chang[1] · Lianpeng Zhang[1] · Yimin Wang[1] · Bo Ming[2]

Received: 26 July 2017 / Accepted: 30 July 2018

Abstract
The watershed hydrological model is regarded as a powerful tool for simulating streamflow, but it is subject to many uncertainties. TOPMODEL (TOPography-based hydrological MODEL) is used as hydrological modeling in this paper; general likelihood uncertainty estimation (GLUE) and multi-criteria GLUE (M-GLUE) methods are applied to evaluate the uncertain effect of model parameters on streamflow simulation, and three climate models are used to investigate the uncertain effect of meteorological input data. A new parameter calibration method (cuckoo search algorithm) is proposed in this study. Taking Beiluo River basin as a study case, analysis of the simulation results reveals that the cuckoo search algorithm is applicable and effective in optimizing the model parameters. The Morris and GLUE methods are employed to analyze the sensitivity of the parameters, and the two methods consistently demonstrated that there are three sensitive parameters in TOPMODEL. Additionally, the results of M-GLUE method are superior to the GLUE method, and both methods can effectively analyze the uncertainty of parameters. The precipitation and potential evaporation predicted by the three climate models exhibit an increasing trend, and the simulated average annual streamflow of the climate system model of the Beijing Climate Center (BCC-CSM1.1) is optimal and followed by Centre National de Recherches Météorologiques Earth system model (CNRM-CM5) and Canadian Earth System Molde (CanESM2). However, results obtained by all the three methods are greater than the baseline period value, indicating that the diverse input data of the hydrological model lead to uncertainty in the streamflow simulation.

1 Introduction

Hydrological model is a simplified description of the rainfall-runoff process in a watershed. Combining the mathematical equations with the parameters which representing the runoff yield and concentration characteristics of a watershed, hydrological models are widely used in hydrological forecasting (Bingeman et al. 2006; Sun et al. 2014a, b; Li et al. 2014; Suliman et al. 2016). To apply the hydrological models to the actual forecasting, determination of parameters is the key step. Numerous researches on hydrological simulation have been performed over the past few decades. In modern flood forecasting, hydrological response to climate change and human activities, eco-hydrological process simulation, and water resources planning and management are widely used. After decades of development, distributed hydrological model has become an important tool for the hydrological simulation. Furthermore, the development of hydrological models took a big step forward after the integration of GIS/RS technology (Gong et al. 2011; Samadi et al. 2013; Dommenget 2016). Due to the simple structure and physical mechanism, TOPMODEL has been widely implemented for terrain analysis and streamflow modeling in regional or global climate models (Schmidt and Persson 2003). However, uncertainties in the simulation and forecasting appeared when using hydrological models (Choi and Beven 2007; Her and Chaubey 2015). Based on the prior distribution of parameters, the GLUE method for evaluating the uncertainty of the hydrological model is used, and the posterior probability distribution of the parameters is deduced by subjectively judging the threshold of the likelihood function of the parameter. The GLUE method does not seek the "best" set of the parameters, but simulates multiple parameter sets to adapt to the uncertainty of model parameters' evaluation; Therefore, the uncertainty range of hydrological simulation with given confidence level is determined. Moreover, the simulated characteristics are described by means of simulated intervals, such as coverage rate (CR), interval width (IW), and interval symmetry

✉ Jianxia Chang
chxiang@xaut.edu.cn

[1] State Key Laboratory of Eco-hydraulics in Northwest Arid Region of China, Xi'an University of Technology, Xi'an, China

[2] State Key Laboratory of Water Resources and Hydropower Engineering Science, Wuhan University, Wuhan 430072, China

Published online: 10 August 2018

(Beven and Freer 2001; Sun et al. 2014a, b; Her and Chaubey 2015). However, due to the objective function, the uncertainty interval of the hydrological process simulation is large. Any single objective function is valid for certain states (such as a high water level) of the hydrological process, but not for other states of the hydrological process (such as a low water level). Hence, various observation data must be used to measure the hydrological process characteristics from different perspectives when selecting parameters of the hydrological model. To address these perspectives, the M-GLUE is more advantageous, as it uses multi-target hydrological model parameters. M-GLUE evaluates the uncertainty of the hydrological model parameters by using likelihood functions which avoid the failure of considering complex hydrological processes inherent in a single objective function.

Parameter calibration is the primary concern in the hydrological model application. At present, the commonly current methods to determine parameters are artificial adjustment. However, the manual adjustment of parameters (Zappa and Kan 2007) is subjective and time-consuming, particularly when multiple objective functions are used (Seibert 2000). As a consequence, a series of automatic calibration methods has been developed, which can avoid human subjectivity and select the optimal parameters from a lot of immediate parameter sets. Simultaneously, large quantity of random parameter sets are tested to find the optimal ones, and then the optimal parameters are manually refined (Konz and Seibert 2010; Hauser et al. 2012). Consequently, the best parameters are obtained by simulating evolution (Seibert 2000). Moreover, a cuckoo search (CS) algorithm is applied to calibrate the parameters of the hydrological model which is rarely used in other studies (Ming et al. 2018a, 2018b). In addition, the combination of the CS algorithm with the hydrological model can find the optimal parameters quickly and accurately while avoiding subjectivity.

The Beiluo river basin (BLR) is the longest tributary of the Weihe River basin (WRB) and is the second-level tributary of the Yellow River basin (YRB). Natural streamflow is the basis for maintaining the balance of a watershed ecosystem and for the sustainable development of society and the economy. Overall, the annual and seasonal precipitation tend to decrease, while temperature shows an increasing trend. The streamflow presents a significant decreasing trend in the WRB over the past few decades (Chang et al. 2015). The streamflow variability in the BLR basin has attracted the attention and interest of local government and academic research. It is important to analyze the impact of climate change on streamflow in the BLR by using hydrological modeling. However, there are still challenges for the local water managers to understand hydrological changes of the BLR.

The combination of the climate model and the hydrological model has a good performance on predicting the future streamflow (Jung and Chang 2011; Solaiman et al. 2011; Okkan and Fistikoglu 2014). This study investigates model simulations based on three GCMs taking part in CMIP5 and combines the climate models with TOPMODEL to analyze the future streamflow changes. Besides, the CS algorithm is used to calibrate the model parameters, and the GLUE and M-GLUE methods are applied to analyze the TOPMODEL parameters uncertainty.

2 Study area and data

The BLR basin, an area of 26,900 km^2 with a length of 680 km, is located in China in the temperate zone at the transition from semi-humid to semi-arid (Fig. 1). The mean annual precipitation is range from 510 to 540 mm. The climatic characteristics are mild, cool, and dry in winter and hot in summer, and the annual mean temperature is 7.5 °C. The average

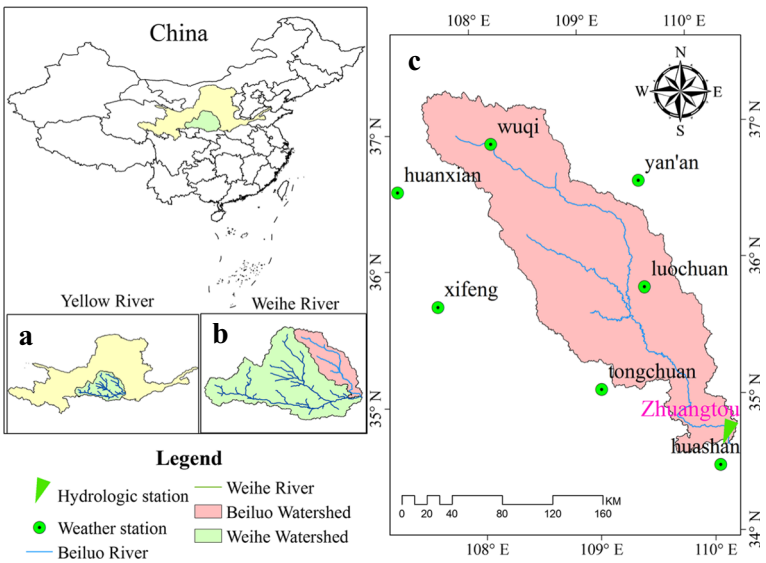

Fig. 1 Location of the study area. **a** The Yellow river of China. **b** The Weihe river basin. **c** the BLR basin. Green dots mean weather stations and green triangle means hydrological station

annual natural streamflow is 8.2×10^8 m^3. Zhuangtou flow gauging station is the outlet station of the BLR.

In this study, the meteorological data (1960–2010), including precipitation, relative humidity, temperature, and wind speed, of seven stations were collected from the China Meteorology Administration. The Digital Elevation Mode (DEM) is provided by the Geospatial Data Cloud of China. Daily streamflow data are collected from the Zhuangtou hydrological station from the Shaanxi Hydrometric and Water Resource Bureau. The Penman-Monteith method is used to estimate the potential evaporation.

3 Methodology

3.1 Hydrological modeling

In this paper, TOPMODEL, a semi-distributed hydrological model proposed by Beven and Kirky in 1979 based on a topographic index, is used as the hydrological model to simulate the streamflow. TOPMODEL is based on the theory of variable flow area, and its main idea focuses on the basis of research on topographic index. When the water content in the aerated zone reaches a saturated water content, the water in the soil becomes free water and flows completely under the action of gravity. Due to the vertical drainage and lateral water movement in the basin, the groundwater level in some basin areas rises to the surface of the ground to become a saturated surface, and the streamflow only occurs on this saturated surface (i.e., the saturated source area). In the whole precipitation process, the source area is constantly changing, and its location is affected by two factors: watershed topography and soil hydraulic characteristics. The TOPMODEL model determines the size and location of the source area by soil moisture content. The soil water shortage (D) is the difference between the soil water content and the saturated water content, and the area of $D_i \leq 0$ is the saturated source area, and saturated surface streamflow will be generated in these areas. The formula for calculating D is as follows:

$$\alpha \frac{\partial j}{\partial x} - \frac{\partial D}{\partial t} = (i - j) \tag{1}$$

where α is the coefficient, j is the flow of the source area, D is the soil water shortage, x is the curve water flow path along the steepest slope, t is the time, and i is the rainfall intensity.

The three basic assumptions of the model are that the hydraulic gradient of saturated groundwater approximates the local topographic slope of the surface, and the soil conductivity is the exponential decreasing function of the water shortage, and the production flow j is spatially equal. According to the above assumptions, the following formula can be obtained:

$$\frac{\overline{D} - D_i}{\mathrm{szm}} = \left[\ln \frac{\alpha}{\tan\beta} - \lambda \right] \tag{2}$$

$$\lambda = \frac{1}{A} \times \sum_i A_i \ln \frac{\alpha}{\tan\beta} \tag{3}$$

where, $\overline{D}$ is the average water shortage, D_i is the water shortage of the ith grid, szm is the rate coefficient when the soil infiltration rate is exponentially decayed, α is the single wide area upstream of the grid, $\tan\beta$ is the surface topography slope, A is the basin area, and $\ln \frac{\alpha}{\tan\beta}$ is called the terrain index.

TOPMODEL has been widely used because of its relatively simple structure and few parameters (Romanowicz and Beven 1998). Many studies have found that TOPMODEL provides a better simulation effect after parameter calibration. TOPMODEL has seven parameters, and the ranges of the TOPMODEL parameters are listed in Table 1 (Van et al. 2013). In recently years, TOPMODEL has been widely applied in humid and semi-humid watersheds, as well as in semi-arid zone basins such as the YRB in China (Lin et al. 2010; Xiong and Guo 2004; Chang et al. 2016). The works demonstrate that this model has a wide range of applications.

3.2 CS, GLUE, and M-GLUE methods

All of the hydrological model parameters must be optimized. In this paper, a CS algorithm is adopted to optimize the TOPMODEL parameters. The CS algorithm is better than

Table 1 Ranges of parameters used by TOPMODEL

Parameter	Unit	Physical meaning	Minimum value	Maximum value	Sampling strategy
SR_{max}	m	Root zone available water storage capacity	0	0.5	Uniform
SR_0	m	Initial stream discharge represented	0.001	0.1	Uniform
M	m	Maximum moisture deficit	0.01	1	Uniform
T_0	m^2 h^{-1}	Transmissivity of the soil profile at full saturation	0	10^2	Uniform
T_d	h	Time parameter	0.01	24	Uniform
R_v	mh^{-1}	Channel flow routing velocity inside catchment	0	2000	Uniform
CH_v	mh^{-1}	Channel and overland flow routing velocity	0	10,000	Uniform

Table 2 Sensitivity level classification

Level	Index	Sensitivity
I	$0.00 \le \lvert S \rvert < 0.05$	Insensitivity
II	$0.05 \le \lvert S \rvert < 0.20$	Average sensitivity
III	$0.20 \le \lvert S \rvert < 1.00$	Moderately high sensitivity
IV	$\lvert S \rvert \ge 1$	High sensitivity

the traditional manual parameter adjustment and can quickly and intelligently calibrate the model parameters. The CS calibration method has the advantages of fast convergence, high convergence accuracy, and less parameters and so on. The significant high efficiency of CS is due to two key mechanisms called Lévy flight random walk and preference random walk and the global and local search of the both balanced algorithm. The CS calibration method has been widely applied in various fields, becoming a new highlight heuristic algorithm following the GA and PSO (Yang and Deb 2014). CS algorithms belong to a heuristic group of intelligent search algorithms that combine cuckoo's nest parasitism with the Lévy flight model. The cuckoos use random walk to search for an optimal bird's nest in which to hatch their eggs. Random walk is an efficient optimization model described by:

$$x_i^{(t+1)} = x_i^{(t)} + \alpha \oplus L(\lambda) \tag{4}$$

$$\alpha = 0.01 \times (x_h - x_l) \tag{5}$$

$$L(\lambda) \sim \mu = t^{-\lambda} \tag{6}$$

$$x_i^{(t+1)} = x_i^{(t)} + \gamma \times H(P_a - \varepsilon) \oplus \left[x_j^{(t)} - x_k^{(t)} \right] \tag{7}$$

where $x_i^{(t)}$ denotes the position of the ith bird's nest in the tth generation, α is the step size, the product $\oplus$ is entry-wise multiplication, $L(\lambda)$ denotes the search step size and obeys Levy distribution, x_h, and x_l are the upper and lower boundaries of the search space, respectively, $H(P_a - \varepsilon)$ denotes a Heaviside function, P_a is the probability that the nest's owner finds the intruding cuckoo, and the default value is 0.25, and γ ε are subjected uniform distributions (Ming et al. 2018a, 2018b; Yang and Deb 2010).

The GLUE method proposed by Beven and Binley (1992) is used to analyze the parameter uncertainty of the hydrological model. For more detailed information on the GLUE method, please refer to Blasone et al. (2008). The GLUE method commonly uses a single objective function.

The M-GLUE method, a multi-criteria likelihood uncertainty estimation, has been proposed as an alternative to GLUE since the use of a single objective function fails to take all the features of the intricate hydrological process into consideration. In addition to the Nash–Sutcliffe efficiency coefficient (NSE) objective function used in the GLUE method, M-GLUE uses the water balance error (WBE) and the total water error (TWE). The CR and IW are used to appraise the M-GLUE method (Lin et al. 2010) according to the following formulas:

$$NSE = 1 - \frac{\sum_{i=1}^{N} \left(Q_{o,i} - Q_{s,i} \right)^2}{\sum_{i=1}^{N} \left(Q_{o,i} - \overline{Q_o} \right)^2} \tag{8}$$

$$WBE = \left| \frac{100 \times \left(\sum_{i=1}^{N} Q_{s,i} - \sum_{i=1}^{N} Q_{o,i} \right)}{\sum_{i=1}^{N} Q_{o,i}} \right| \tag{9}$$

$$TWE = \frac{\sum_{i=1}^{N} \left| Q_{o,i} - Q_{s,i} \right|}{\sum_{i=1}^{N} Q_{o,i}} \times 100\% \tag{10}$$

$$CR = \frac{\sum_{i=1}^{N} J\left[Q_{o,i} \right]}{N} \times 100, J\left[Q_{o,i} \right] = \left\{ \begin{matrix} 1, Q_{L,i} < Q_{0,i} < Q_{U,i} \\ 0, other \end{matrix} \right\} \tag{11}$$

$$IW = \frac{\sum_{i=1}^{N} \left(Q_{U,i} - Q_{L,i} \right)}{N} \tag{12}$$

where $Q_{o,\,i}$, $Q_{s,\,i}$, $\overline{Q_o}$, $Q_{L,\,i}$, and $Q_{U,\,i}$ denote the observed streamflow, simulated streamflow, the monthly average streamflow, and the lower and upper streamflow, respectively. N is the total number of data.

3.3 Morris method

The Morris method (Morris 1991) is a qualitative method of global sensitivity analysis, which is usually applied to recognize sensitive parameters. The fundamental principle of the Morris method is the evaluation of the output change corresponding to a small change in a single factor. Sensitivity can be partitioned into the four levels described in Table 2. The sensitivity evaluation index from Morris method is as follows:

$$S = \sum_{i=0}^{n-1} \left[\frac{(Y_{i+1} - Y_i)/Y_0}{(P_{i+1} - P_i)/P_i} \right] / (n-1) \tag{13}$$

where S denotes the sensitivity evaluation index; Y_{i+1} and Y_i are the simulation values at times $i+1$ and i, respectively; Y_0 is the initial simulation value; P_{i+1} and P_i denote the change rate of the simulation value with respect to the optimal value, and n is the number of the simulation run times.

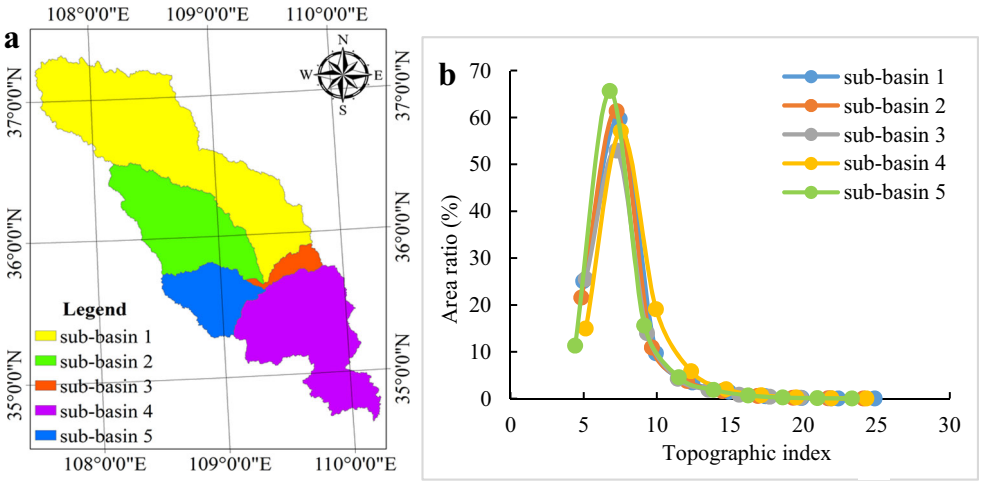

Fig. 2 Information for five sub-basins. **a** The sub-basin location. **b** The sub-basin's topographic index distribution, and the ordinate means the corresponding area ratio of the topographic index

3.4 Modeling climate variables and the SDSM method

CMIP5 is the global-coupled ocean-atmosphere circulation model (Taylor et al. 2012; Siew et al. 2014; Qu et al. 2014). CMIP5 provides meaningful and useful datasets for evaluation and discussion of global and regional climate changes (Torres and Marengo 2014). In this paper, the RCP4.5 and RCP8.5 scenario datasets of three climate models (BCC-CSM1.1, CanESM2, and CNRM-CM5) are used to analyze the uncertainty of the input data. Because the grid resolution is different for the three climate models, CMIP5's grid resolution is adjusted to the resolution of the National Centers for Environment Prediction data via the Inverse Distance Weighted method. The Statistical Down Scaling Model (SDSM) uses a robust statistical downscaling technique to assess the impacts of climate change. For a detailed description of the SDSM, please refer to Huang et al. (2012). In this paper, outputs from the three climate models (BCC-CSM1.1, CanESM2, and CNRM-CM5) are input to SDSM to simulate monthly precipitation and potential evaporation from 1960 to 2050. Then, the generated data are input to TOPMODEL to simulate future streamflow under different climate scenarios.

4 Results and discussion

4.1 Parameters' calibration based on the CS algorithm

The DEM data are handled by ArcGIS software. As shown in Fig. 2, the BLR basin is divided into five different sub-basins because of the large area, and the topography index and area ratio distribution of each sub-basin are calculated. The Mann-Kendall (M-K) test is used to analyze the breakpoint of the streamflow. As shown in Fig. 3, the breakpoint of the streamflow series appears in 1995. Therefore, based on the breakpoint result, 1960–1977 and 1978–1994 are selected as the calibration period and the validation period of hydrological model simulation, respectively. The input data of the model are the monthly precipitation and potential evapotranspiration, and the parameters of the model are determined by the CS algorithm. The parameters of each sub-basin are shown in Table 3. The CS algorithm, given 10 nests and run 300 times, is applicable and can quickly and effectively optimize the parameters. For the calibration and validation periods, the observed streamflow and the simulated streamflow by using CS

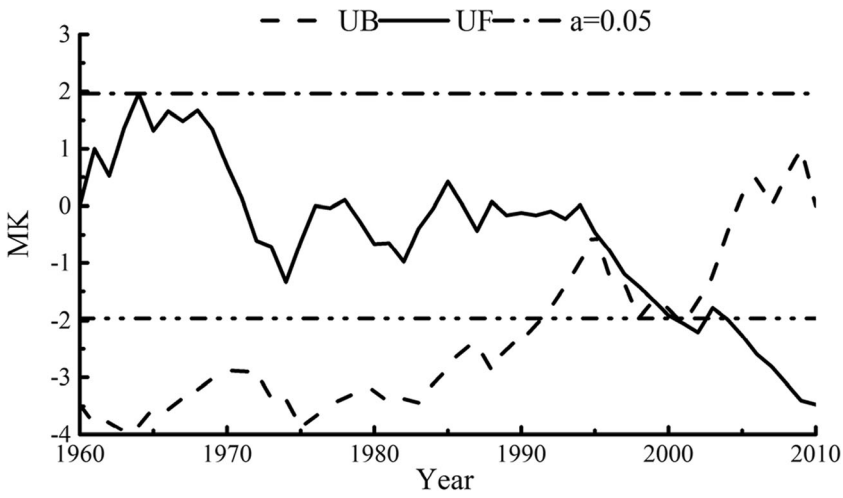

Fig. 3 The streamflow breakpoint test by using the M-K method. UF is the order statistic of the streamflow sequence, and UB is the reverse statistic of the sequence. $a = 0.05$ is the level of significance, that is, the thresholds of the UF and UB are ± 1.96. The intersection of UB and UF is the breakpoint

Table 3 Parameters of TOPMODEL optimized by the CS algorithm

Sub-basin	T_0	M	T_d	s	R_v	CH_v	SR_0
1	2.200	0.012	0.080	0.009	995	6000	0.001
2	0.098	1.380	0.900	0.010	1000	15	0.001
3	0.001	2.400	0.097	0.006	24	10	0.001
4	0.008	2.540	2.500	0.017	500	4100	0.001
5	0.003	2.270	0.076	0.018	200	17	0.001

algorithm optimized parameters are shown in Fig. 4. In this paper, the NSE and WBE are adopted as objective functions, and the NSE (WBE) values are 0.77 (5.34%) and 0.62 (6.23%) in calibration and validation periods, respectively.

4.2 Uncertainty analysis of the model parameters

4.2.1 Sensitivity analysis of the model parameters

The Morris method is used to analyze the parameters sensitivity, and the results are shown in Table 4. There are three sensitive parameters, namely, R_v, SR_{max} and CH_v. The GLUE method is applied to test the parameters' sensitivity again, and Fig. 5 shows that R_v, SR_{max} and CH_v are sensitive in the range of parameter variation. The scatter diagrams of the other three parameters, however, show that the variation of these parameters is not obvious. This result is consistent with the Morris parameter screening method analysis. Therefore, R_v, SR_{max}, and CH_v are sensitive parameters that have significant influence on the simulation results, so this paper presents further analysis of the influence of these three parameters on the simulation results.

Table 4 Sensitivity of the TOPMODEL parameters

No.	Parameters	Sensitivity	Level
1	M	0.128	II
2	T_0	− 0.017	I
3	SR_{max}	− 0.551	III
4	SR_0	0	I
5	T_d	0.185	II
6	R_v	− 0.598	III
7	CH_v	− 0.522	III

4.2.2 Uncertainty analysis of the model parameters based on GLUE and M-GLUE

This section presents the uncertainty analysis of the three parameters. First, 10,000 sets of parameters are obtained at random by the GLUE method, and the threshold value of the likelihood function is set to 0.7. Then, all the parameters above this threshold value (effective parameter group) are selected and sorted according to their likelihood values. Finally, setting the confidence level to 90% ($\alpha = 0.5$), the uncertainty interval of the streamflow simulation value is calculated. The minimum and maximum values (Table 5) are consistent with the ranges of the parameters, indicating that the parameter space is searched effectively. Figure 6 shows the marginal posterior probability distributions of the sensitive parameters in the BLR basin using the GLUE method. At each time step, the vertical coordinates correspond to the probability that the parameter value falls between the current scale value and the previous scale value. No parameters are uniformly distributed, and they exhibit large uncertainties.

Although the marginal posterior distributions of sensitivity parameters are obtained through the GLUE method, since the

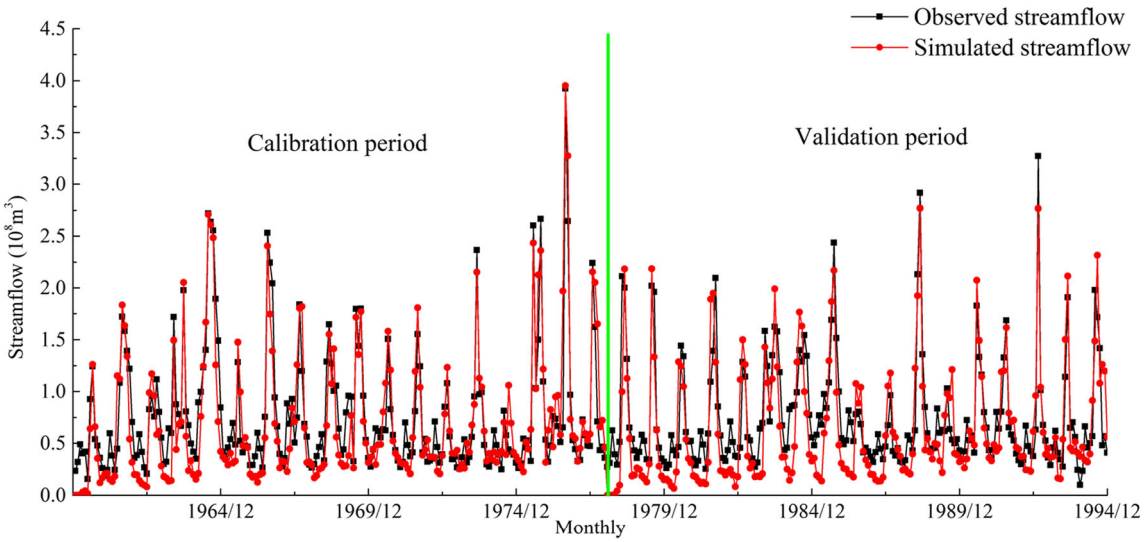

Fig. 4 Comparison for the observed monthly streamflow and the simulated monthly streamflow. The period to the left of the green line is the calibration period (1960–1977), and the right is the validation period (1978–1994) of TOPMODEL

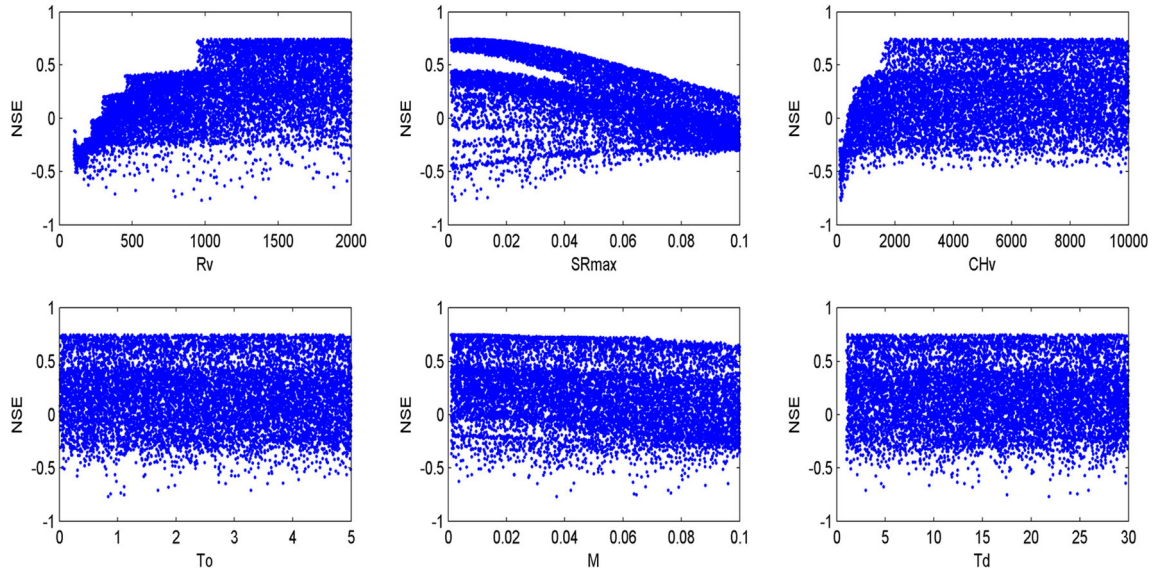

Fig. 5 Scatter plots for model parameters of TOPMODEL. The blue dots mean the values by random operating of each parameter for 10,000 times, and the NSEs are the corresponding likelihood function values

model exhibits very strong "equifinality," in the actual process of hydrological forecasting, the results are truly meaningful. It is not any single parameter that makes the model significant but the combination of the model parameters. In this paper, the convergence of the 420 sets of effective parameters generated by the GLUE method is selected to simulate streamflow and to generate the statistics concerning the 90% confidence interval ($\alpha = 0.5$) of the streamflow forecast. It can be seen (Fig. 7) that majority of the observed streamflow falls within the 90% confidence interval. The CR and IW of the GLUE method are 77.31% and 0.79×10^8 m^3 in the calibration period, respectively, and in the validation period, they are 50.98% and 0.18×10^8 m^3 (Table 6).

To avoid the single-factor evaluation index of the GLUE method, the M-GLUE method is applied to analyze the uncertainty of the model parameters. It can be seen (Fig. 7) that the CR and IW of the GLUE method are 80.56% and 0.75×10^8 m^3, respectively, during the calibration period, and in the validation period, they are 74.51% and 0.34×10^8 m^3 (Table 6). The similarity between the 90% confidence interval obtained by M-GLUE method and measured streamflow is greater than that of the GLUE method, which indicates that the uncertainty of the M-GLUE method simulation is reduced in comparison to GLUE. For the M-GLUE method, three criteria (NSE, WBE, and TWE) are used to construct the evaluation index, rather than a single criterion, which improves the overall accuracy and reduces the simulation error. Then, the convergence of the 177 sets of effective parameters are generated by the M-GLUE method (the GLUE method is 420 sets). When selecting the same effective number of simulations, although the average NSE of GLUE (0.71) is slightly lower than that of M-GLUE (0.73), the 90% confidence interval of M-GLUE is obviously superior to that of the GLUE method. In the calibration period, the CR of the M-GLUE method is obviously better than that of the GLUE method. The difference is approximately 10%, which indicates that the uncertainty interval of the M-GLUE method is less than that of GLUE. It can also be seen from the IW values that the IW of the M-GLUE method is smaller than that of the GLUE method. These two criteria show that increasing the likelihood function can reduce the uncertainty of the model output. In the validation period, although the IW of the M-GLUE method is wider than that of the GLUE method, the M-GLUE CR is obviously higher than that of the GLUE method. A larger IW value result may due to comprehensively balancing the different likelihood function and slightly widening the range of the likelihood function, but the CR improvement is far greater than the adverse effects on IW. Accordingly, the M-GLUE method outperforms the GLUE method. Therefore, it is feasible to adopt M-GLUE method in this paper to analyze the uncertainty of the parameters of TOPMODEL model in the BLR basin.

Table 5 The posterior distribution of parameters

Parameters	Mean	Standard deviation	Minimum	Maximum
SR_{max}	0.01	0.006	0.001	0.03
CH_v	6022	2301	1662	9954
R_v	1552	289	944	1999

4.3 Uncertainty analysis of model inputs

In the presence of climate change, many climate variables will change. The changes in the meteorological data of the BLR basin derived from the RCP4.5 and RCP8.5 scenarios of three

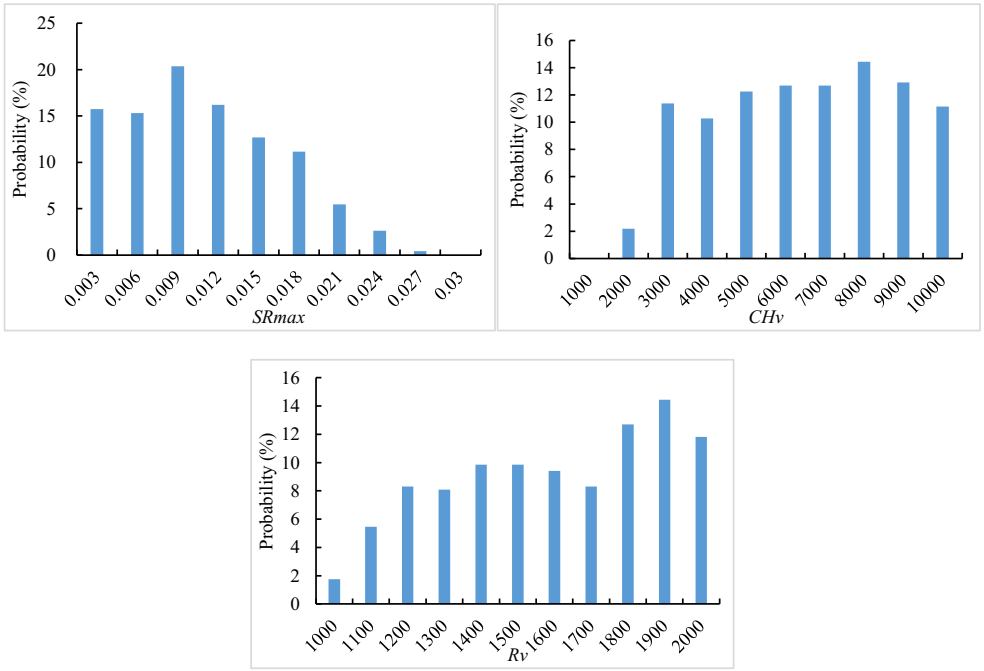

Fig. 6 Probabilities histograms for three sensitive parameters. The ordinate means the probability that the parameter value falls between the current scale value and the previous scale value

models and the streamflow simulated thereafter are presented in the figures below. The series mean values for baseline period (2000–2010) and future periods under different climate scenarios are calculated. The M-K method is used to examine the breakpoint of the streamflow, and the existed breakpoint shows the non-stationary of the streamflow. Therefore, the

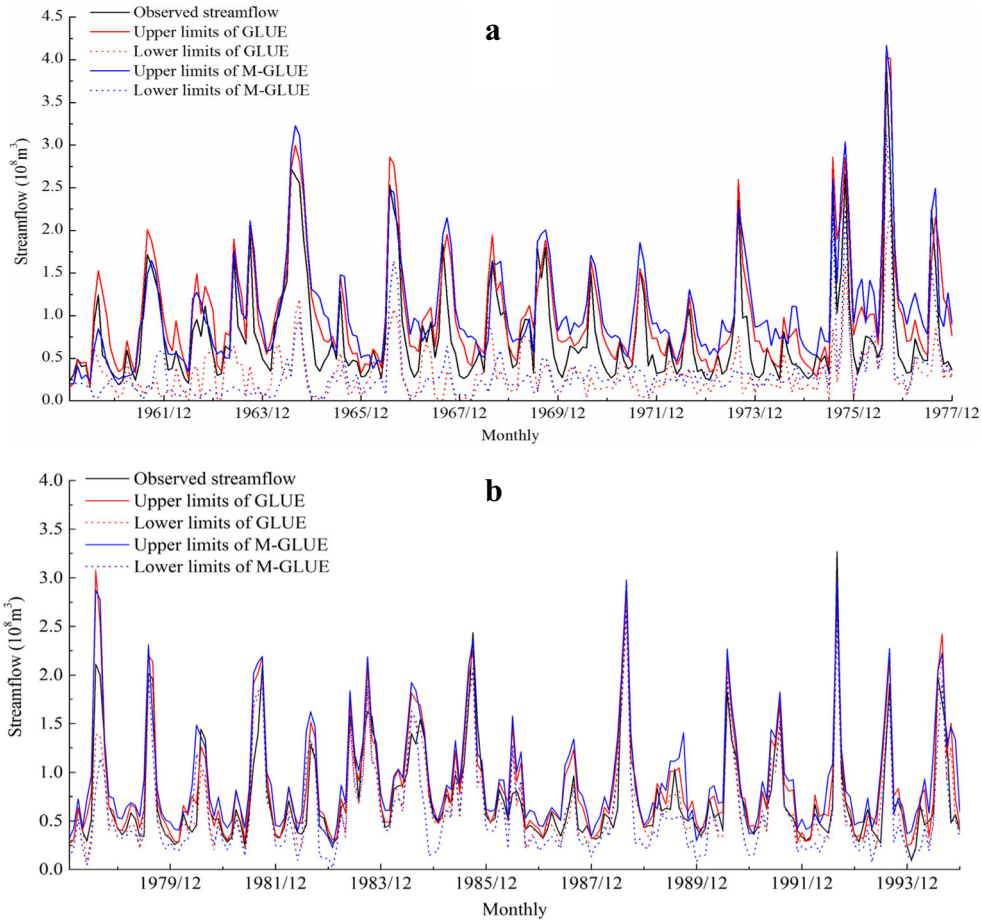

Fig. 7 The upper and lower limits (90% confidence interval) of streamflow calculated by the GLUE and M-GLUE methods. **a** The result of calibration period (1960–1977). **b** The result of validation period (1978–1994)

Table 6 Comparison of two methods of discriminant criteria

Classification	Calibration period		Validation period	
	CR (%)	IW (10^8 m^3)	CR (%)	IW (10^8 m^3)
S-GLUE	77.31	0.79	50.98	0.18
M-GLUE	80.56	0.75	74.51	0.34

streamflow before the breakpoint cannot be selected to simulate the future streamflow. The breakpoint of streamflow is 1995, so, the 2000~2006 was selected as the calibration period and the 2007~2010 as the validation period, which are shown in Fig. 8. The results show that the simulated NSE and WBE are 0.899 and 0.17 in calibration period, respectively, and in validation period are 0.765 and 0.22. Therefore, the validated parameter group can be applied in the future streamflow simulation of BLR.

Figure 9 shows the relative changes in precipitation and potential evaporation for the 2020s (2016–2030), 2030s (2031–2040), and the 2040s (2041–2050) in comparison with the baseline period of the three models. Although the precipitation is predicted to decrease 4.02 mm by the CanESM2 model in the 2020s under RCP8.5, it is predicted to increase by the remaining models, and the increase range is from 13.78 to 93.69 mm. The monthly precipitation fluctuates in all scenarios (Fig. 9). The maximum monthly precipitation appears in August in the BCC-CSM1.1 and CNRM-CM5 models (except during the 2020s in the CNRM-CM5 model), while it appears in July in the CanESM2 model. The minimum precipitation values appear in winter (December to February). The precipitation in August in the BCC-CSM1.1 model is significantly higher than that in the baseline period, and the predicted annual average precipitation in future time periods is also higher than those for the other two models. The three models predict annual average potential evaporation to increase in all future scenarios and the increase range is from 18.21 to 109.90 mm. The highest increases in potential evaporation are predicted under RCP8.5. The monthly potential evaporation from August to February of next year is higher than that for the baseline period. The maximum monthly potential evaporation appears in June under two scenarios of the three models; the exception appears in July under the RCP8.5 scenario of the BCC-CSM1.1 model. In the winter, the minimum monthly potential evaporation appears in January or December.

To analyze the impact of climate change on streamflow in the future, the streamflow under each climate change scenarios is compared with baseline period values. The simulated annual streamflows in the future and baseline periods are shown in Fig. 10a–c). The annual simulated streamflows under two scenarios of the three climate models are greater than that of the baseline period (8.2×10^8 m^3), and the annual simulated streamflow shows a decreasing trend over time (Fig. 10). Using the BCC-CSM1.1 model, the maximum

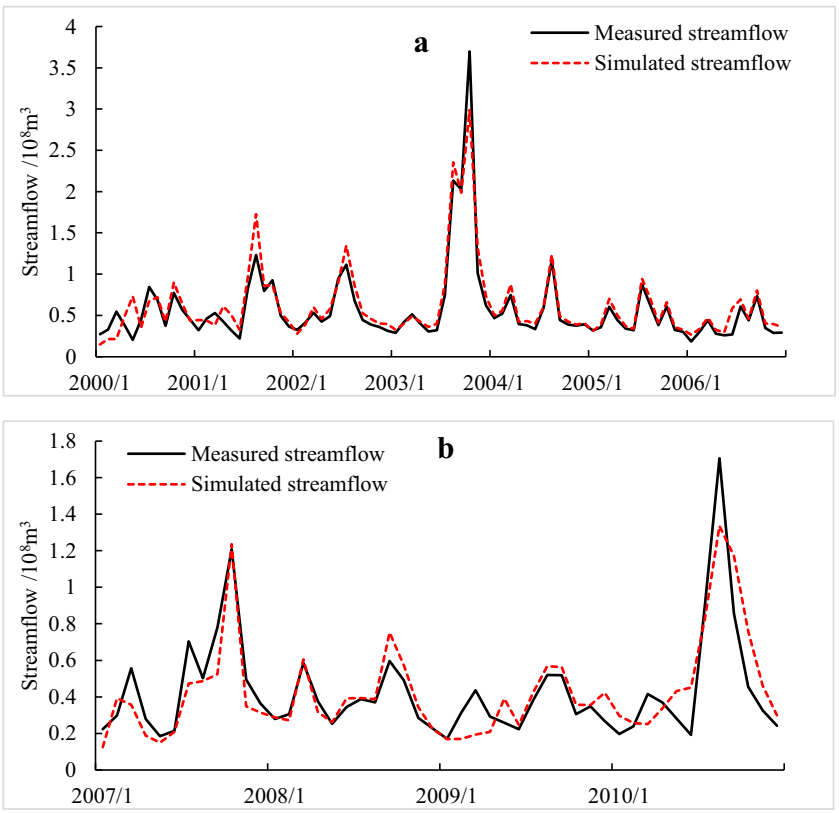

Fig. 8 Comparison for the monthly observed streamflow and the monthly simulated streamflow from TOPMODEL. **a** The result of calibration period (2000–2006). **b** The result of validation period (2007–2010)

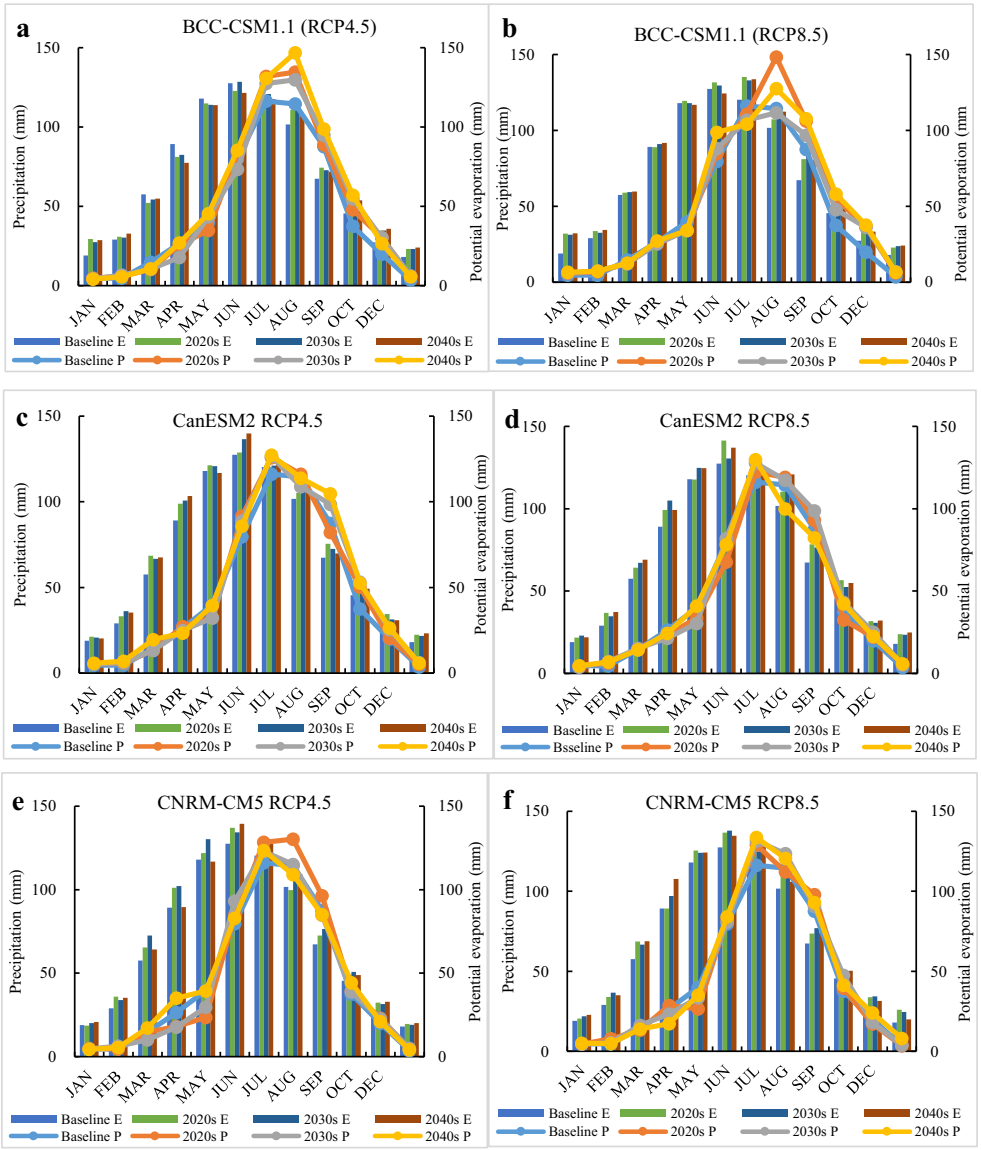

Fig. 9 The monthly precipitation (P) and monthly potential evaporation (E) during the baseline period (2000–2010) and three future periods (2020s, 2030s, and 2040s). **a**, **b** The results under scenarios RCP4.5 and RCP8.5 from BCC-CSM1.1 model. **c**, **d** The results under scenarios RCP4.5 and RCP8.5 from CanESM2 model. **e**, **f** The results under scenarios RCP4.5 and RCP8.5 from CNRM-CM5 model

annual streamflow appears in 2022 under two scenarios (13.1×10^8 m^3 and 12.3×10^8 m^3), but their minimum streamflows occur in different years (Table 7). The mean annual simulated streamflow of the RCP8.5 scenario (9.63×10^8 m^3) is greater than that of the RCP4.5 scenario (10.42×10^8 m^3). For the CanESM2 model, the maximum annual streamflows of the RCP4.5 and RCP8.5 scenarios appear in 2046 (10.09×10^8 m^3) and 2042 (9.86×10^8 m^3), respectively,

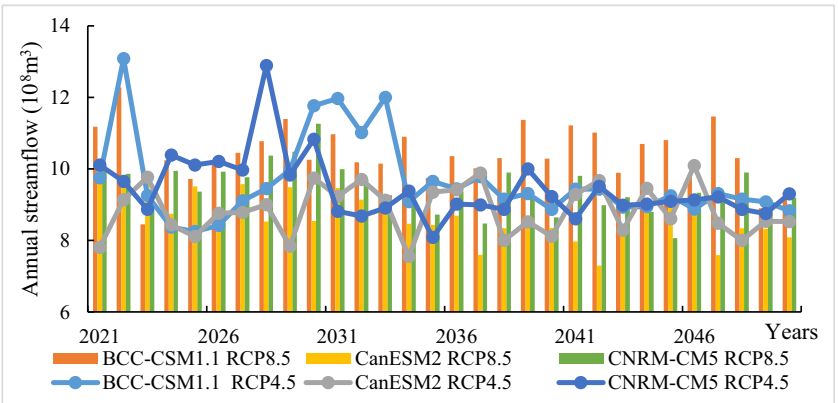

Fig. 10 The simulated annual streamflow during future periods (2021–2050) of three models. The bar charts mean the results under scenarios RCP4.5, and the line charts mean the results under scenarios RCP8.5

Table 7 Streamflow statistics of the baseline and three climate models

Models	Maximum annual streamflow occurrence time		Minimum annual streamflow occurrence time	Mean annual streamflow/10^8 m^3	The increment of streamflow /10^8 m^3
Baseline		–	–	8.20	–
BCC-CSM1.1	RCP4.5	2022	2025	9.63	1.43
	RCP8.5	2022	2023	10.42	2.22
CanESM2	RCP4.5	2016	2034	8.84	0.64
	RCP8.5	2021	2042	8.72	0.52
CNRM-CM5	RCP4.5	2028	2035	9.44	1.24
	RCP8.5	2030	2045	9.46	1.26

and the minimum ones appear in 2034 (7.55×10^8 m^3) and 2042 (7.29×10^8 m^3). The mean annual simulated streamflows of the RCP4.5 and RCP8.5 scenarios differ very little, 8.84×10^8 m^3 and 8.72×10^8 m^3, respectively. For the CNRM-CM5 model, the maximum annual streamflows of the RCP4.5 and RCP8.5 scenarios appear in 2028 (12.89×10^8 m^3) and 2030 (11.26×10^8 m^3), respectively, and the minimum ones appear in 2035 (8.08×10^8 m^3) and 2045 (8.06×10^8 m^3). The mean annual simulated streamflows of the RCP4.5 and RCP8.5 scenarios also differ very little and are 9.44×10^8 m^3 and 9.46×10^8 m^3, respectively.

In summary, the maximum annual streamflow occurrence time differs in the three models and the simulated streamflows under the different climate models are diverse. For the average annual streamflow, the simulation streamflow of the BCC-CSM1.1 model is the greatest, followed by that of the CNRM-CM5 model, and CanESM2 has the least simulated streamflow, but they were all greater than the baseline period value, which indicates that diverse data input to the hydrological model will lead to uncertainty in the streamflow simulation. This phenomenon may result from the differences inherent in the three models. The models have been developed by three different research and development centers, and the differences in concepts, mechanisms, and component models (pavement and sea surface) result in different meteorological factors, causing diversity in the simulated precipitation and potential evaporation results and lead to uncertainty in the input data of the hydrological model.

5 Conclusions

The hydrological model fills an important role in simulating streamflow, and the model's uncertainty, regarded as a knotty problem, has been puzzling researchers. A new calibration method for the hydrological model is proposed, and an analysis of the uncertainty in the model's parameters and input data is undertaken in this paper.

(1) The CS algorithm is applicable and effective in optimizing the model parameters. The Morris and GLUE methods are employed to analyze the sensitivity of the parameters, and the two methods consistently demonstrated that there are three sensitive parameters in TOPMODEL, namely, R_v, SR_{max}, andCH_v.

(2) The GLUE and M-GLUE methods can effectively analyze the uncertainty of parameters, and the 90% confidence interval of streamflow could be forecast. The values of CR and IW in the calibration period are77.31% and 0.79×10^8 m^3 with the GLUE method, respectively, and that are 80.56% and 0.75×10^8 m^3 with the M-GLUE method, respectively. Additionally, the results of M-GLUE method are superior to the results of GLUE method.

(3) Precipitation and potential evaporation are predicted by the three GCMs, and the results indicate that these characteristics show an increasing trend. Then, the future streamflow of the models are simulated to analyze the effect of uncertainty in model input data on simulated streamflow. The maximum annual streamflow occurrence times are different for the three models, and the simulated streamflow under the different climate models is diverse. In the case of average annual streamflow, the simulation streamflow of the BCC-CSM1.1 model is optimal and followed by CNRM-CM5 and CanESM2 model. However, results obtained by all the three methods are higher than the baseline period value, indicating that diverse hydrological model input data cause uncertainty in the streamflow simulation.

These results have important practical significance and scientific value for the calibration of the hydrological parameters, the evaluation of the uncertainty of the model, and for the exploration of new ideas for future comprehensive management of river basin water resources. The reasonable selection of the model calibration method can reduce the resource management workload, and an effective uncertainty analysis method can reduce the uncertainty of simulation results.

Funding information This research was supported by the National Natural Science Foundation of China (91647112 and 51679187) and the National Key Research and Development Program of China (2016YFC0400906). Many thanks to the China Meteorology Administration and the Shaanxi Hydrometric and Water Resource Bureau for providing research data.

References

Beven K, Binley A (1992) The future of distributed models: model calibration and uncertainty prediction. Hydrol Process 6(3):279–298

Beven KJ, Freer J (2001) Equifinality, data assimilation, and uncertainty estimation in mechanistic modelling of complex environmental systems using the GLUE methodology. J Hydrol 249(1–4):11–29

Blasone RS, Vrugt JA, Madsen H, Rosbjerg D, Robinson BA, Zyvoloski GA (2008) Generalized likelihood uncertainty estimation (GLUE) using adaptive Markov Chain Monte Carlo sampling. Adv Water Resour 31(4):630–648

Bingeman AK, Kouwen N, Soulis ED (2006) Validation of the hydrological processes in a hydrological model. J Hydrol Eng 11(5):451–463

Chang J, Wang Y, Istanbulluoglu E, Bai T, Huang Q, Yang D, Huang S (2015) Impact of climate change and human activities on runoff in the Weihe River basin, China. Quat Int 380:169–179

Chang J, Zhang H, Wang Y, Zhu Y (2016) Assessing the impact of climate variability and human activities on streamflow variation. Hydrol Earth Syst Sci 20(4):1547–1560

Choi HT, Beven K (2007) Multi-period and multi-criteria model conditioning to reduce prediction uncertainty in an application of TOPMODEL within the GLUE framework. J Hydrol 332(3):316–336

Dommenget D (2016) A simple model perturbed physics study of the simulated climate sensitivity uncertainty and its relation to control climate biases. Clim Dyn 46(1–2):427–447

Gong Y, Shen Z, Hong Q, Liu R, Liao Q (2011) Parameter uncertainty analysis in watershed total phosphorus modeling using the GLUE methodology. Agric Ecosyst Environ 142(3):246–255

Hauser T, Keats A, Tarasov L (2012) Artificial neural network assisted Bayesian calibration of climate models. Clim Dyn 39(1–2):137–154

Her Y, Chaubey I (2015) Impact of the numbers of observations and calibration parameters on equifinality, model performance, and output and parameter uncertainty. Hydrol Process 29(19):4220–4237

Huang J, Zhang J, Zhang Z, Sun S, Yao J (2012) Simulation of extreme precipitation indices in the Yangtze River basin by using statistical downscaling method (SDSM). Theor Appl Climatol 108(3–4):325–343

Jung IW, Chang H (2011) Assessment of future runoff trends under multiple climate change scenarios in the Willamette River basin, Oregon, USA. Hydrol Process 25(2):258–277

Konz M, Seibert J (2010) On the value of glacier mass balances for hydrological model calibration. J Hydrol 385(1):238–246

Li B, Su H, Chen F, Li H, Zhang R, Tian J, Chen S, Yang Y, Rong Y (2014) Separation of the impact of climate change and human activity on streamflow in the upper and middle reaches of the Taoer River, northeastern China. Theor Appl Climatol 118(1–2):271–283

Lin K, Zhang Q, Chen X (2010) An evaluation of impacts of DEM resolution and parameter correlation on TOPMODEL modeling uncertainty. J Hydrol 395(3):370–383

Ming B, Liu P, Guo S, Cheng L, Zhou Y, Gao S, Li H (2018a) Robust hydroelectric unit commitment considering integration of large-scale photovoltaic power: a case study in China. Appl Energy 228: 1341–1352

Ming B, Liu P, Cheng L, Zhou Y, Wang X (2018b) Optimal daily generation scheduling of large hydro–photovoltaic hybrid power plants. Energy Convers Manag 171:528–540

Morris MD (1991) Factorial sampling plans for preliminary computational experiments. Technometrics 33(2):161–174

Okkan U, Fistikoglu O (2014) Evaluating climate change effects on runoff by statistical downscaling and hydrological model GR2M. Theor Appl Climatol 117(1–2):343–361

Romanowicz R, Beven K (1998) Dynamic real-time prediction of flood inundation probabilities. Hydrol Sci J 43(2):181–196

Samadi S, Wilson CAME, Moradkhani H (2013) Uncertainty analysis of statistical downscaling models using Hadley Centre coupled model. Theorectical Appl Climatol 114(3–4):673–690

Schmidt F, Persson A (2003) Comparison of DEM data capture and topographic wetness indices. Precis Agric 4(2):179–192

Seibert J (2000) Multi-criteria calibration of a conceptual runoff model using a genetic algorithm. Hydrol Earth Syst Sci Discuss 4(2):215–224

Siew JH, Tangang FT, Juneng L (2014) Evaluation of CMIP5 coupled atmosphere–ocean general circulation models and projection of the southeast Asian winter monsoon in the 21st century. Int J Climatol 34(9):2872–2884

Solaiman TA, King LM, Simonovic SP (2011) Extreme precipitation vulnerability in the upper Thames River basin: uncertainty in climate model projections. Int J Climatol 31(15):2350–2364

Suliman AHA, Katimon A, Darus IZM, Shahid S (2016) TOPMODEL for streamflow simulation of a tropical catchment using different resolutions of ASTER DEM: optimization through response surface methodology. Water Resour Manag 30(9):3159–3173

Sun S, Chen H, Ju W et al (2014a) Assessing the future hydrological cycle in the Xinjiang Basin, China, using a multi-model ensemble and SWAT model. Int J Climatol 34(9):2972–2987

Sun N, Hong B, Hall M (2014b) Assessment of the SWMM model uncertainties within the generalized likelihood uncertainty estimation (GLUE) framework for a high-resolution urban sewershed. Hydrol Process 28(6):3018–3034

Taylor KE, Stouffer RJ, Meehl GA (2012) An overview of CMIP5 and the experiment design. Bull Am Meteorol Soc 93(4):485–498

Van den Putte A, Govers G, Leys A, Langhans C, Clymans W, Diels J (2013) Estimating the parameters of the Green–Ampt infiltration equation from rainfall simulation data: why simpler is better. J Hydrol 476:332–344

Xiong L, Guo S (2004) Effects of the catchment runoff coefficient on the performance of TOPMODEL in rainfall-runoff modeling. Hydrol Process 18(10):1823–1836

Yang XS, Deb S (2010) Engineering optimisation by cuckoo search. Int J Math Model Numer Optimisation 1(4):330–343

Yang XS, Deb S (2014) Cuckoo search: recent advances and applications. Neural Comput Appl 24(1):169–174

Zappa M, Kan C (2007) Extreme heat and runoff extremes in the Swiss Alps. Nat Hazards Earth Syst Sci 7(3):375–389